

# Connecting the cosmic gamma-ray burst rate and star-formation rate with Bayesian analysis of Swift GRBs



Anjali Mittu<sup>1</sup>, John Baker<sup>2</sup>, Amy Lien<sup>2,3,4</sup>

<sup>1</sup>University of Maryland, College Park, MD USA <sup>2</sup>NASA GSFC, Greenbelt, MD, USA

<sup>3</sup>CRSST <sup>4</sup>University of Maryland, Baltimore County Baltimore, MD, USA

## Background

Gamma-ray bursts (GRBs) are some of the most energetic events in the known universe; in just a couple of seconds, GRBs release more than  $10^{51}$  ergs. Because of this, GRBs remain luminous even at high redshift, making them one of the few objects seen at redshifts  $z > 6$ . There are two types of GRBs observed: long GRBs and short GRBs, which are divided based on their light curve and duration. Short GRBs are thought to come from the merger of two compact objects such as neutron stars, while long GRBs come from the core collapse of a massive star.

GRBs are particularly important for studying star formation rate (SFR). At high redshifts, tracing the SFR is very difficult due to the fact that it is hard to see out so far. This results in rates differing by more than an order of magnitude. GRBs should be able to trace SFR since they:

- Can be seen at high redshifts
- Are the result of the death of a massive star

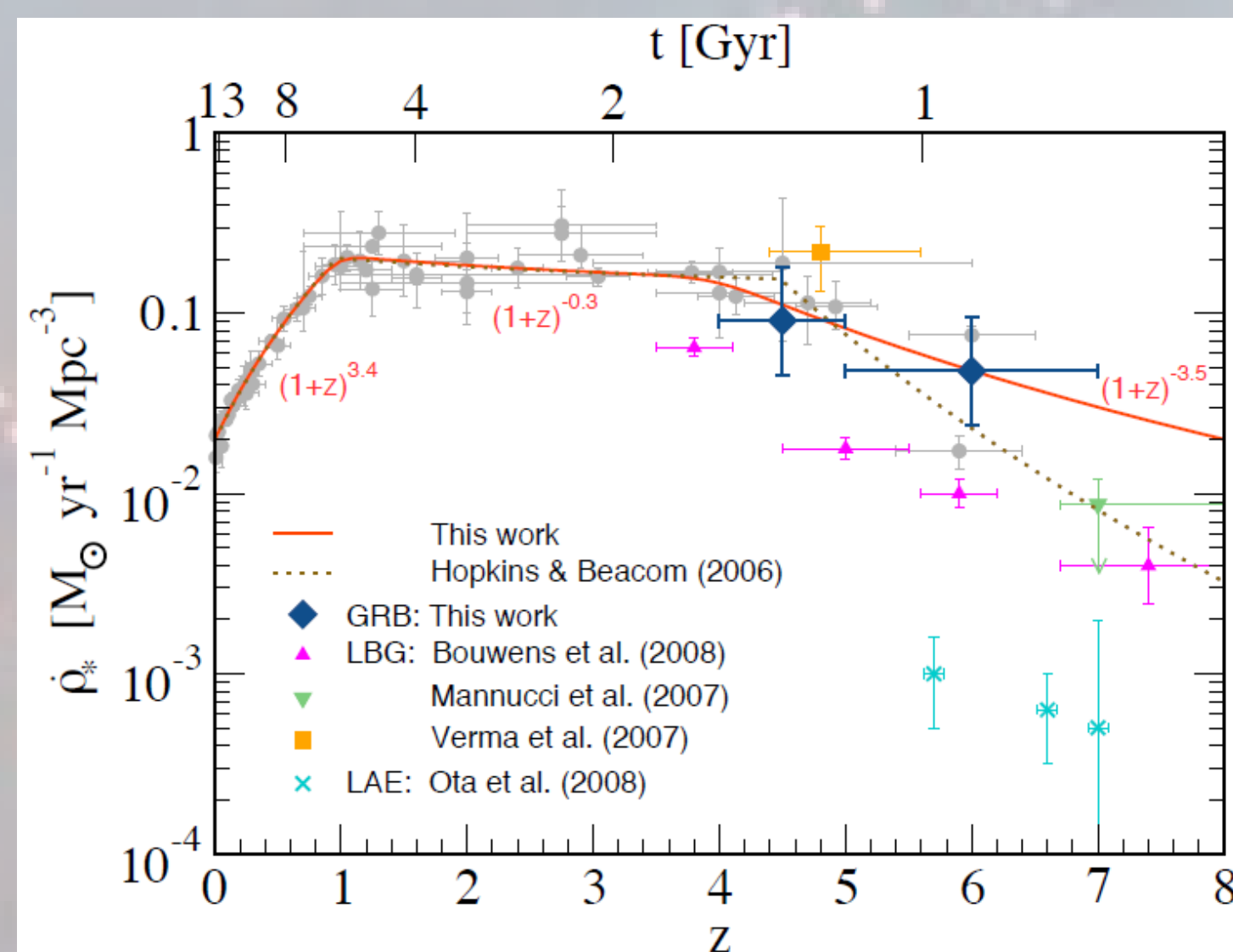


Figure 1: Compiled SFR data from Yüksel et al. (2008)

## Swift Challenge

The burst alert telescope (BAT) on Swift uses a trigger algorithm with >500 criteria based on photon count rate, and additional image threshold for localization. This complex trigger algorithm successfully increases the number of GRBs detected, yet makes estimating the detection fraction more difficult. The complex trigger algorithm introduces selection effects on GRBs. Previous studies usually estimate the trigger algorithm using a flux detection threshold. This might not be a good estimate since each BAT trigger criterion adopts different signal-to-noise ratio threshold.

In this study we applied a fast emulator for the trigger algorithm using four different machine learning algorithms (MLAs):

- random forest
- boosted decision trees
- support vector machines
- artificial neural networks.

Figure 2 shows the results of the detection fraction.

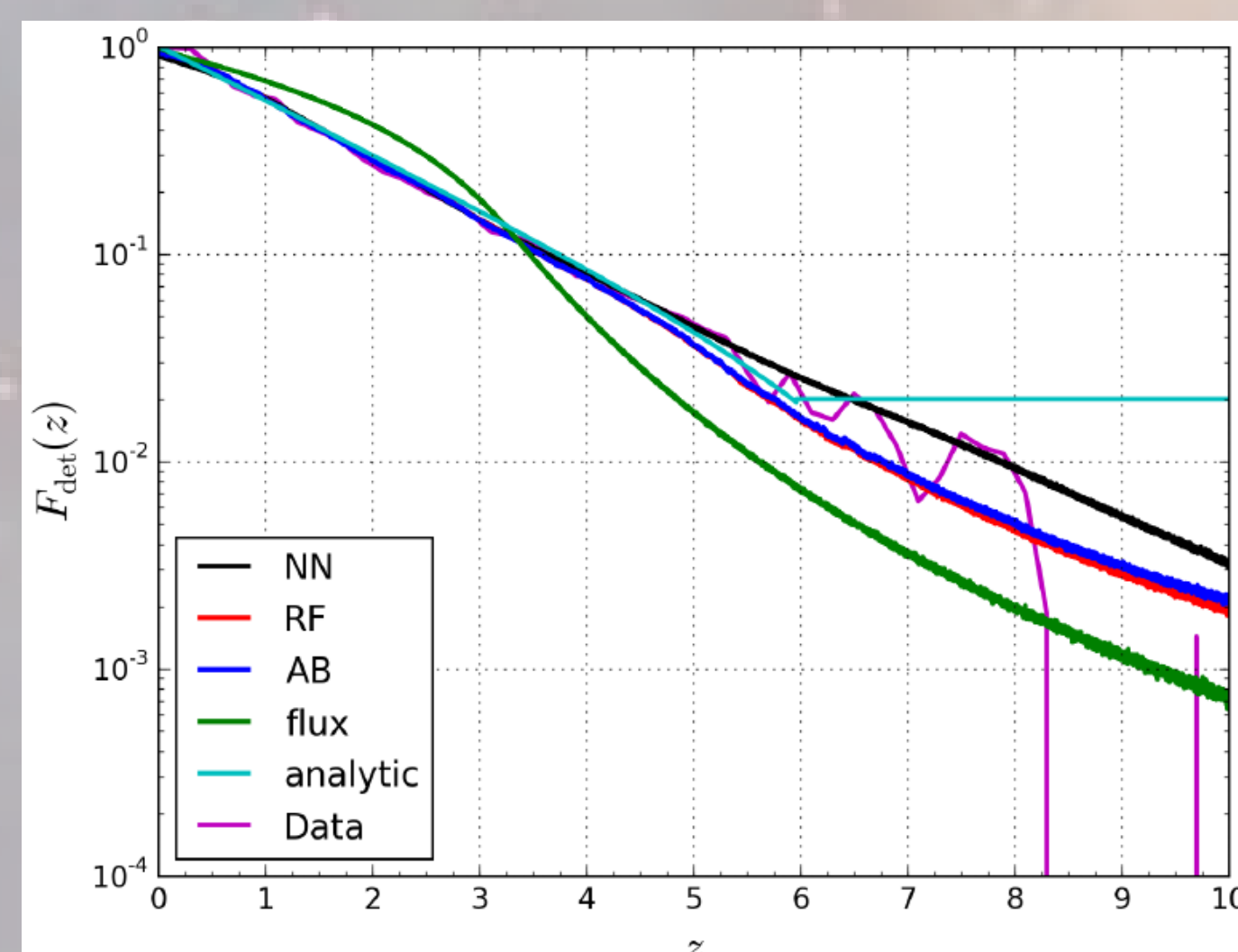


Figure 2: (Graff et al. 2015)  $F_{det}(z_i)$  computed for three different MLAs with the constant flux cut and analytic form used in Howell et al (2014)

## Likelihood Function

The number of intrinsic GRBs occurring in Swift's field of view is given by Equation 1. Where the factor of  $\frac{4\pi}{6}$  accounts that Swift can only observe a sixth of the sky at any time.  $\Delta t_{obs} = 0.8$  which is the amount of time Swift spends observing per year.  $R_{GRB;dz}$  is the GRB rate per redshift per solid angle accounting for time dilation and comoving volume.

$$N_{int}(z_i) = \frac{4\pi}{6} \Delta t_{obs} R_{GRB;dz}(z_i) dz \quad \text{Equation 1}$$

The expected number of observed GRBs comes from multiplying Equation 1 by the detection fraction (which was derived from the Swift emulator).

$$N_{exp}(z_i) = N_{int}(z_i) F_{det}(z_i) = \frac{4\pi}{6} \Delta t_{obs} R_{GRB;dz}(z_i) F_{det}(z_i) dz \quad \text{Equation 2}$$

Since the data is expected to have a Poisson distribution, the log-likelihood is found to be Equation 3, where  $\{i\}_{det}$  is each detection.

$$\mathcal{L}(\vec{n}) = -N_{exp} + \sum_{\{i\}_{det}} \log(N_{exp}(z_i)) \quad \text{Equation 3}$$

For a full deviation see Graff et al. (2015)

## Acknowledgements and References

I would like to thank my mentors John Baker and Amy Lien for all of their guidance and help.

Bouwens R, Illingworth G, Franx M, Ford H. 2008. *Astrophysical Journal*. 686(1):230-250  
 Graff P, Feroz F, Hobson M, Lasenby A. 2012. *Monthly Notices of the Royal Astronomical Society*.  
 Graff P, Lien A, Baker J, Sakamoto T. 2015. *ApJ*. 818(1):55  
 Hopkins A, Beacom J. 2006. *ApJ*. 651(1):142-154  
 Lien A, Sakamoto T, Gehrels N, Palmer D, Barthelmy S et al. 2014. *ApJ*. 783(1):24  
 Mannucci, F., et al. 2007, A&A, 461, 423  
 Ota, K., et al. 2008, ApJ, 677, 12  
 Verma, A., et al. 2007, MNRAS, 377, 1024  
 Yüksel H, Kistler M, Beacom J, Hopkins A. 2008. *ApJ*. 683(1):L5-L8

## One-Break and Two-Break Models

$$R_{GRB}(z) = n_0 \begin{cases} (1+z)^{n_1}, & z \leq z_1 \\ (1+z_1)^{n_1-n_2} (1+z)^{n_2}, & z > z_1 \end{cases} \quad \text{Equation 4}$$

$$R_{GRB}(z) = n_0 \begin{cases} (1+z)^{n_1}, & z \leq z_1 \\ (1+z_1)^{n_1-n_2} (1+z)^{n_2}, & z_1 < z \leq z_2 \\ (1+z_2)^{n_2-n_3} (1+z_1)^{n_1-n_2} (1+z)^{n_3}, & z > z_2 \end{cases} \quad \text{Equation 5}$$

Equation 4 gives the one-break equation for the comoving GRB rate in units of  $Gpc^{-3} yr^{-1}$ , while Equation 5 gives the two-break equation for the comoving GRB rate. The variables  $n_1$  and  $z_1$  used in Equation 1 and Equation 2 were allowed to vary. The ranges and prior distributions of these variables are given in Table 1 and Table 2.

The BAMBI algorithm (Graff et al. 2012) was used to perform the Bayesian parameter estimates on the variables. Table 3 and Table 4 shows the results of the analysis.

The posterior distribution of the parameters shown in Figure 3 and Figure 4 use real data samples of 66 GRBs from Swift and the detection fraction found from the random forest MLA. The dashed red line shows the maximum likelihood value from Table 2 and Table 3. The dashed black lines show the 5%, 50%, and 95% quantiles.

Figure 5 and Figure 6 shows the distribution of the model parameters. The top graph plots the max likelihood  $R_{GRB}(z)$ , while the lower plots max likelihood  $N_{exp}(z)/dz$ . Both of these are shown in black. The blue lines show 200 models with randomly chosen parameters from the posterior. In the lower plot, the dashed line shows the maximum likelihood for  $N_{int}(z)/dz$  and the red boxes show the distribution of observed GRB. The evidence value for the one-break model was 99.43 +/- 0.0441 and the two break was 99.23 +/- 0.0450. The Bayesian analysis does not find preference for either model, and thus does not support the additional complexity of the two-break model, which tends to mimic the results of the one break model.

Parameter	Method	Max Like	90% CI
$n_0$	RF	.513	[0.247, 0.895]
	AB	.523	[0.246, 0.915]
	NN	.405	[0.235, 0.988]
$n_1$	RF	1.656	[1.141, 2.265]
	AB	1.635	[1.154, 2.269]
	NN	1.864	[1.025, 2.351]
$n_2$	RF	-5.997	[-5.668, -0.224]
	AB	-5.942	[-5.686, 0.252]
	NN	-.333	[-5.608, 0.218]
$z_1$	RF	6.70	[3.612, 9.612]
	AB	6.694	[3.617, 9.591]
	NN	3.439	[3.186, 9.402]
$N_{exp}$	RF	4434	[2952, 6844]
	AB	4370	[2965, 6794]
	NN	3414	[2532, 5509]

Table 2: Maximum likelihood estimates and central 90% credible intervals for the one-break redshift distribution parameters

Parameter	Min	Max
$n_0$	0.01	2.00
$n_1$	0.00	4.00
$n_2$	-6.00	6.00
$n_3$	-10.00	0.00
$z_1$	0.00	10.00
$z_2$	0.00	10.00

Table 3: Prior ranges and distributions for the two-break GRB rate parameters

Parameter	Method	Max Like	90% CI
$n_0$	RF	.411	[0.229, 0.908]
	AB	.420	[0.225, 0.908]
	NN	.383	[0.215, 0.971]
$n_1$	RF	1.878	[1.101, 2.400]
	AB	1.859	[1.098, 2.469]
	NN	1.906	[1.011, 2.545]
$n_2$	RF	.978	[-5.185, 4.680]
	AB	.836	[-5.150, 4.532]
	NN	.0954	[-5.148, 3.869]
$n_3$	RF	-8.804	[-9.463, -0.474]
	AB	-9.167	[-9.488, -0.520]
	NN	-9.697	[-9.502, -0.459]
$z_1$	RF	3.403	[1.451, 8.423]
	AB	3.553	[1.305, 8.353]
	NN	3.246	[1.385, 7.927]
$z_2$	RF	6.600	[5.261, 9.800]
	AB	6.804	[5.222, 9.818]
	NN	6.675	[4.468, 9.759]
$N_{exp}$	RF	3919	[2965, 6894]
	AB	3955	[2893, 6839]
	NN	3096	[2536, 5366]

Table 4: Maximum likelihood estimates and central 90% credible intervals for the two-break redshift distribution parameters

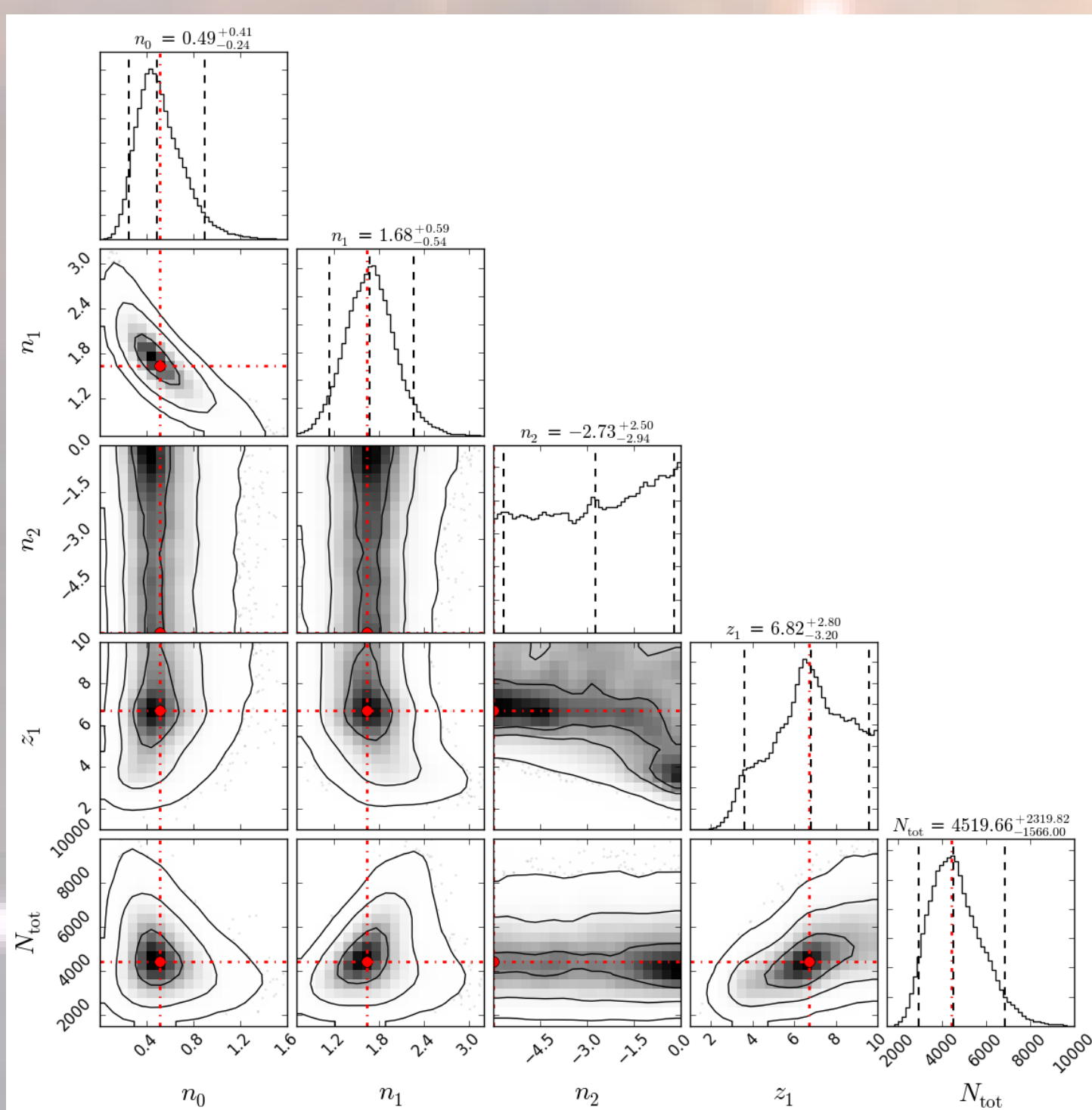


Figure 3: Posterior distribution for the 66 GRBs from Swift using random forest for the one-break model.

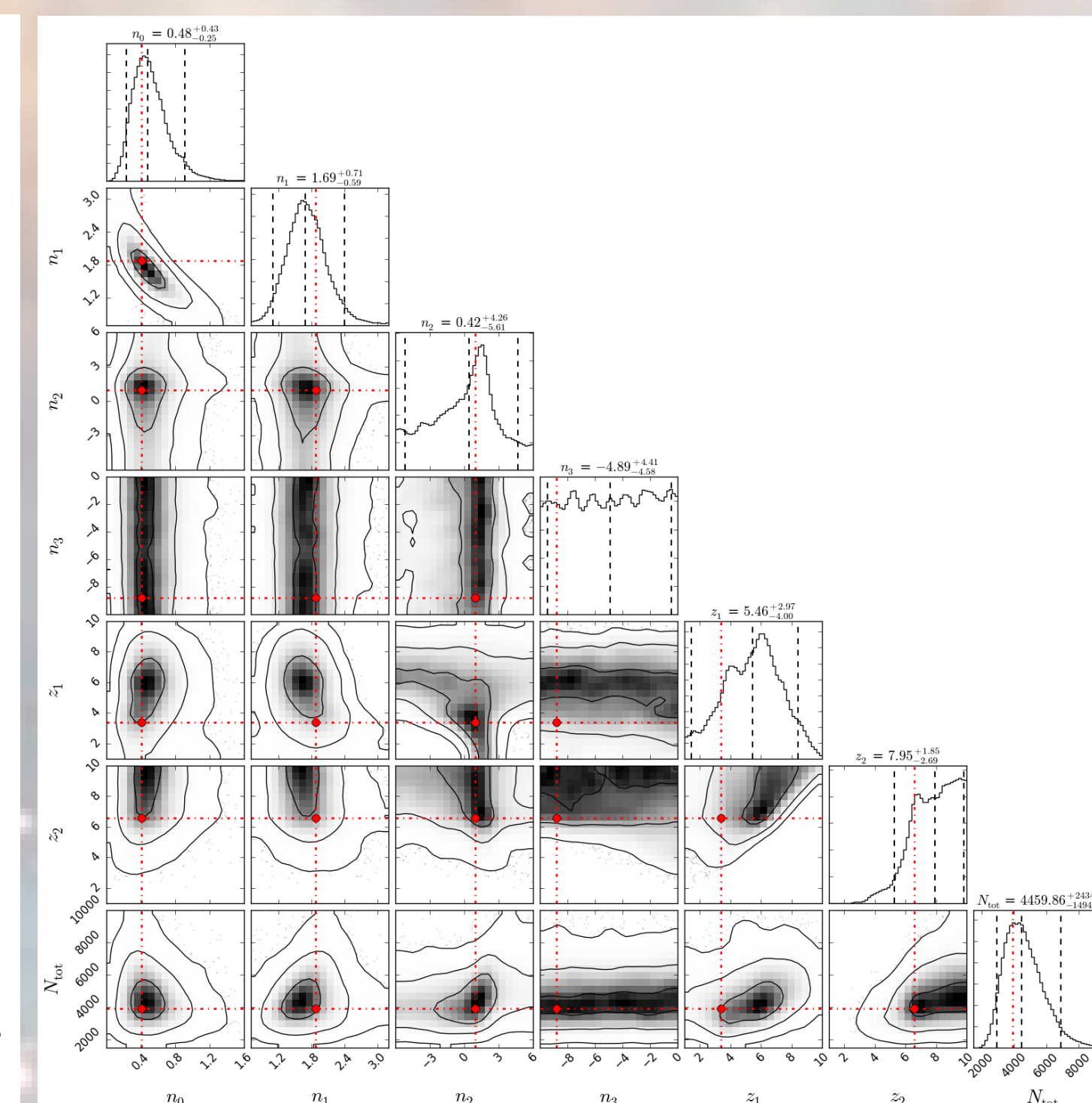


Figure 4: Posterior distribution for the 66 GRBs from Swift using random forest for the two-break model.

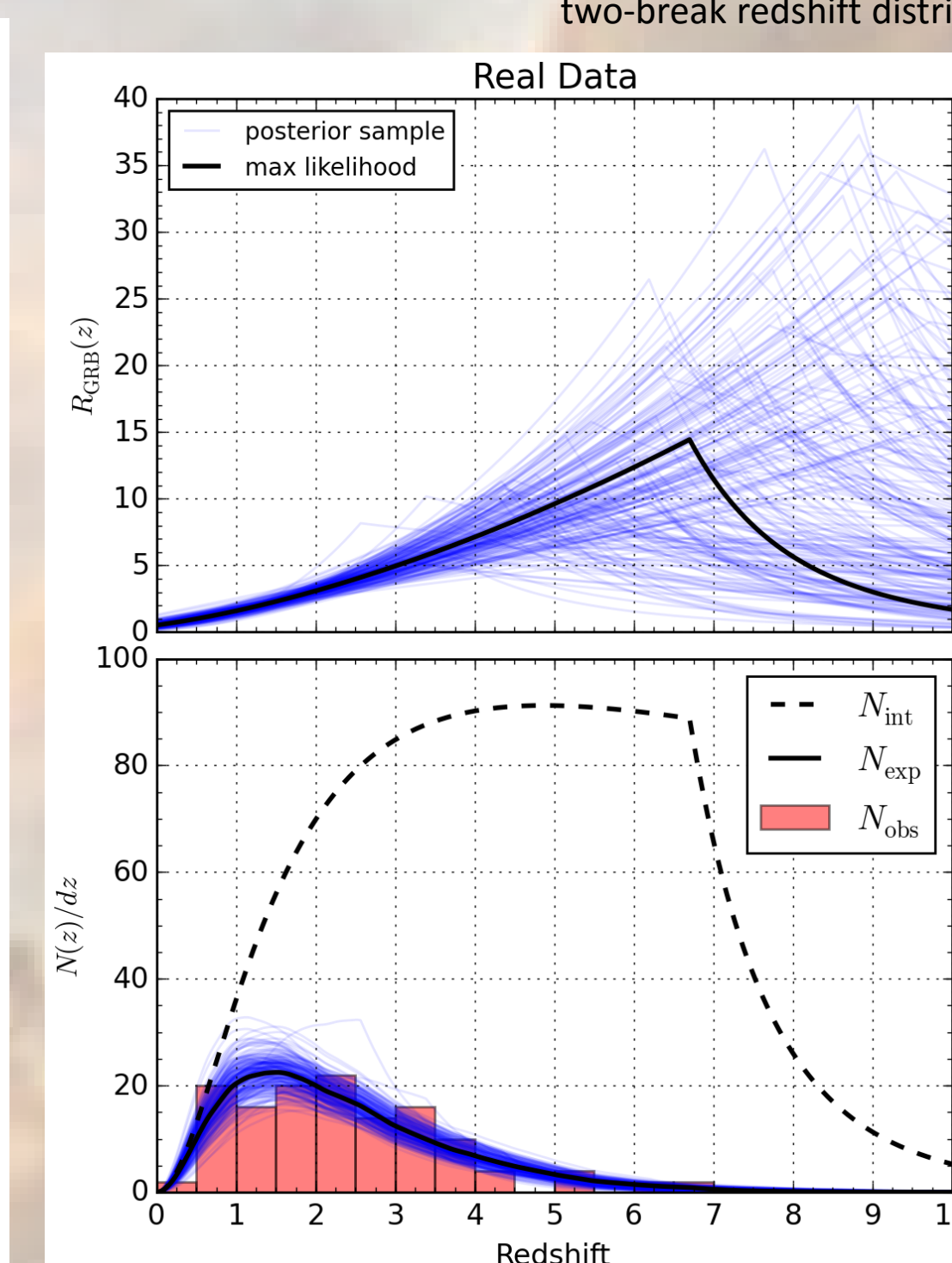


Figure 5: The distribution of the one-break model parameters for the plots of  $R_{GRB}(z)$ , and  $N_{exp}(z)/dz$

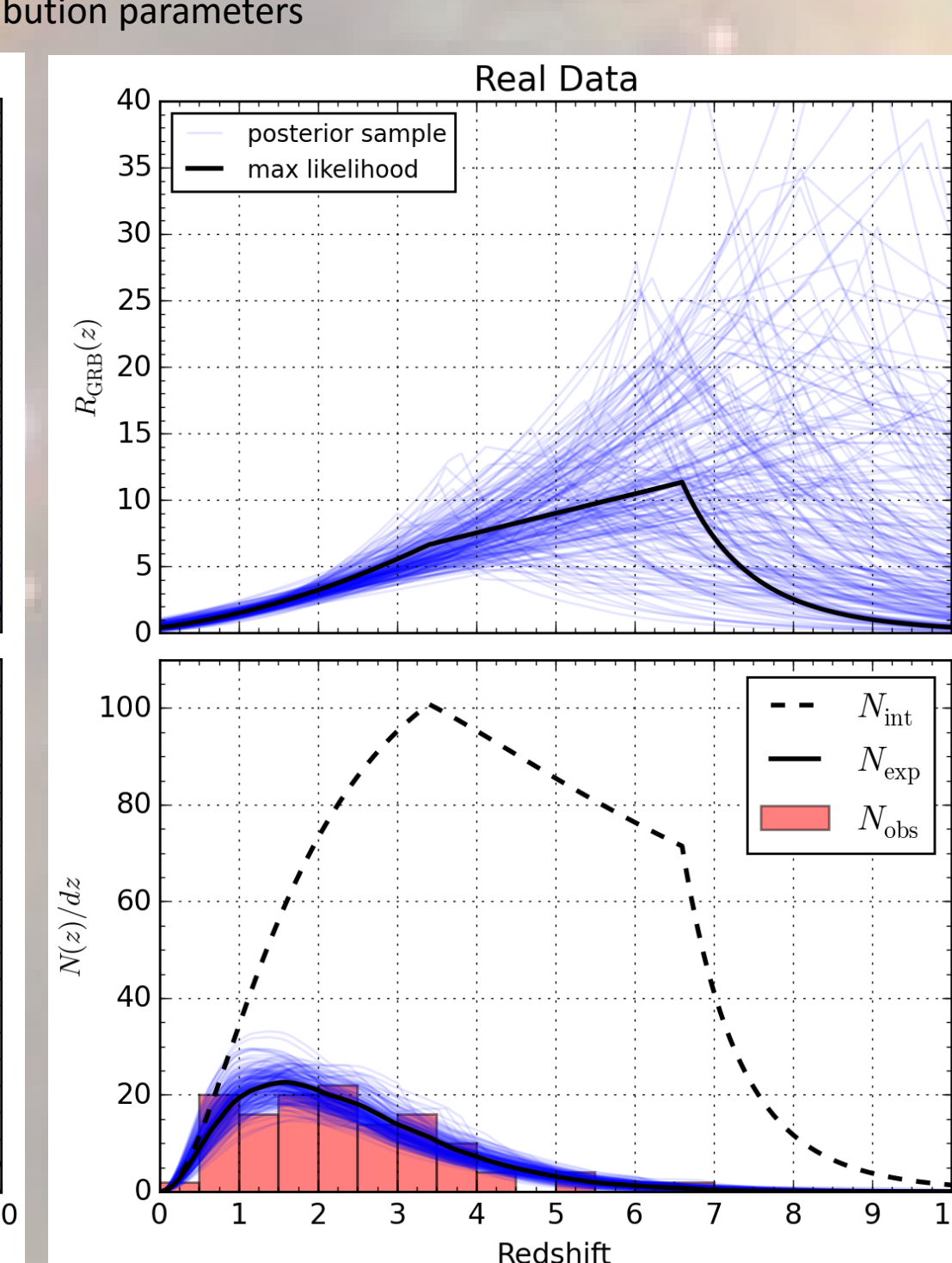


Figure 6: The distribution of the two-break model parameters for the plots of  $R_{GRB}(z)$ , and  $N_{exp}(z)/dz$

## Star Formation Rate Model

I ran a two-break model proportional to the SFR as found in Hopkins and Beacom (2008) by using their parameters  $\{n_1, n_2, n_3, z_1, z_2\} = \{3.28, -0.26, -8.0, 1.04, 4.48\}$  and varying  $n_0$ . The results of this analysis are shown in Figure 7. The likelihood of this model was far less than my one-break or two-break; 84.22 vs. 99.43 and 99.23. In this case the Bayesian evidence does show a strong preference for the one-break model over the model proportional to the SFR.

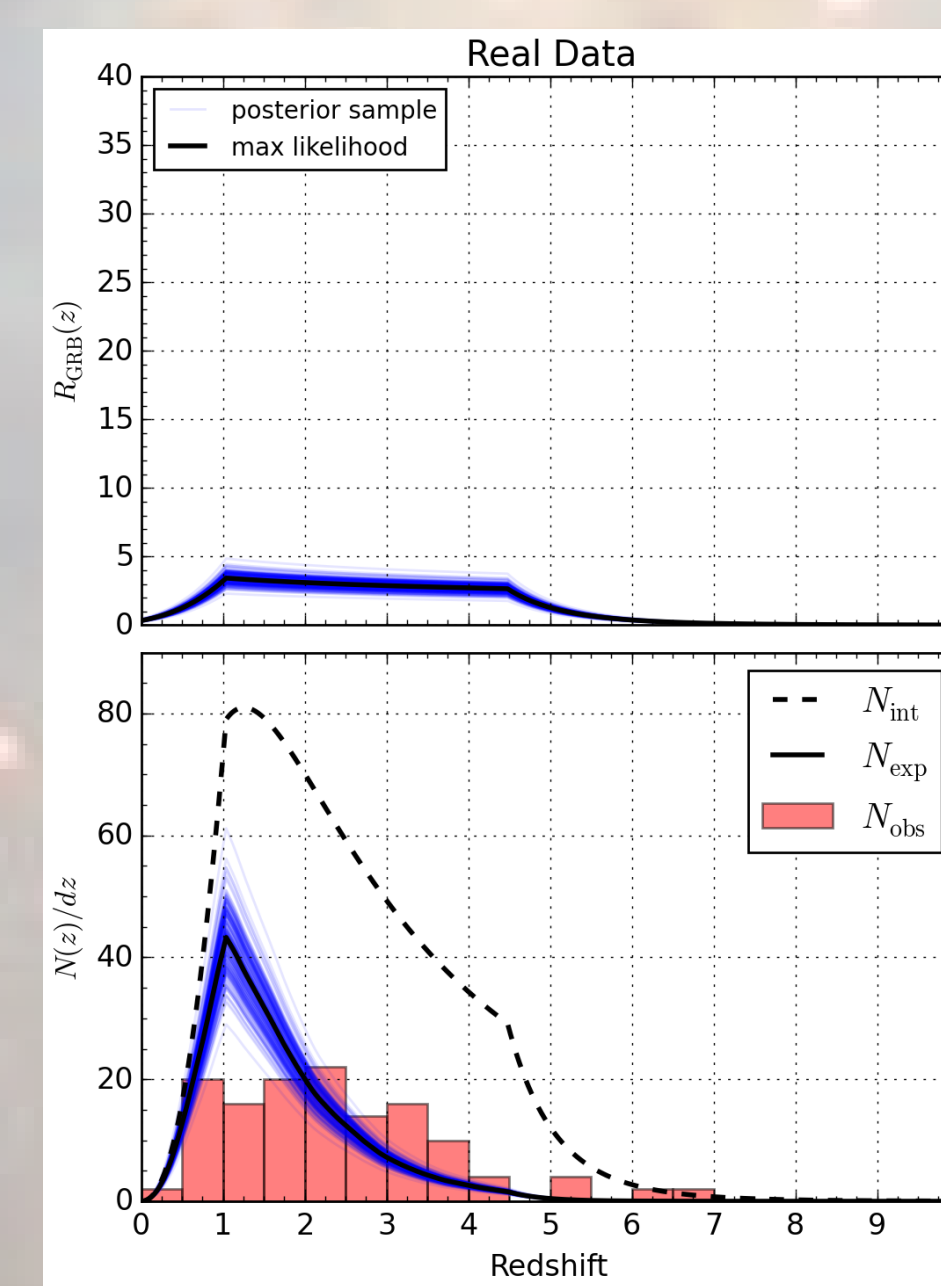


Figure 7: The distribution of the  $n_0$  parameter using Hopkins and Beacom's values. Similar to Figure 4.

Figure 8 shows the max likelihood  $R_{GRB}(z)$  for the one-break and two-break model as well as the fit I found using Hopkins and Beacom's parameters. Along with these three graphs are the GRB rate found in Lien et al (2014) and the GRB rates following SFR from Hopkins and Beacom (2006) and Yüksel et al. (2008).

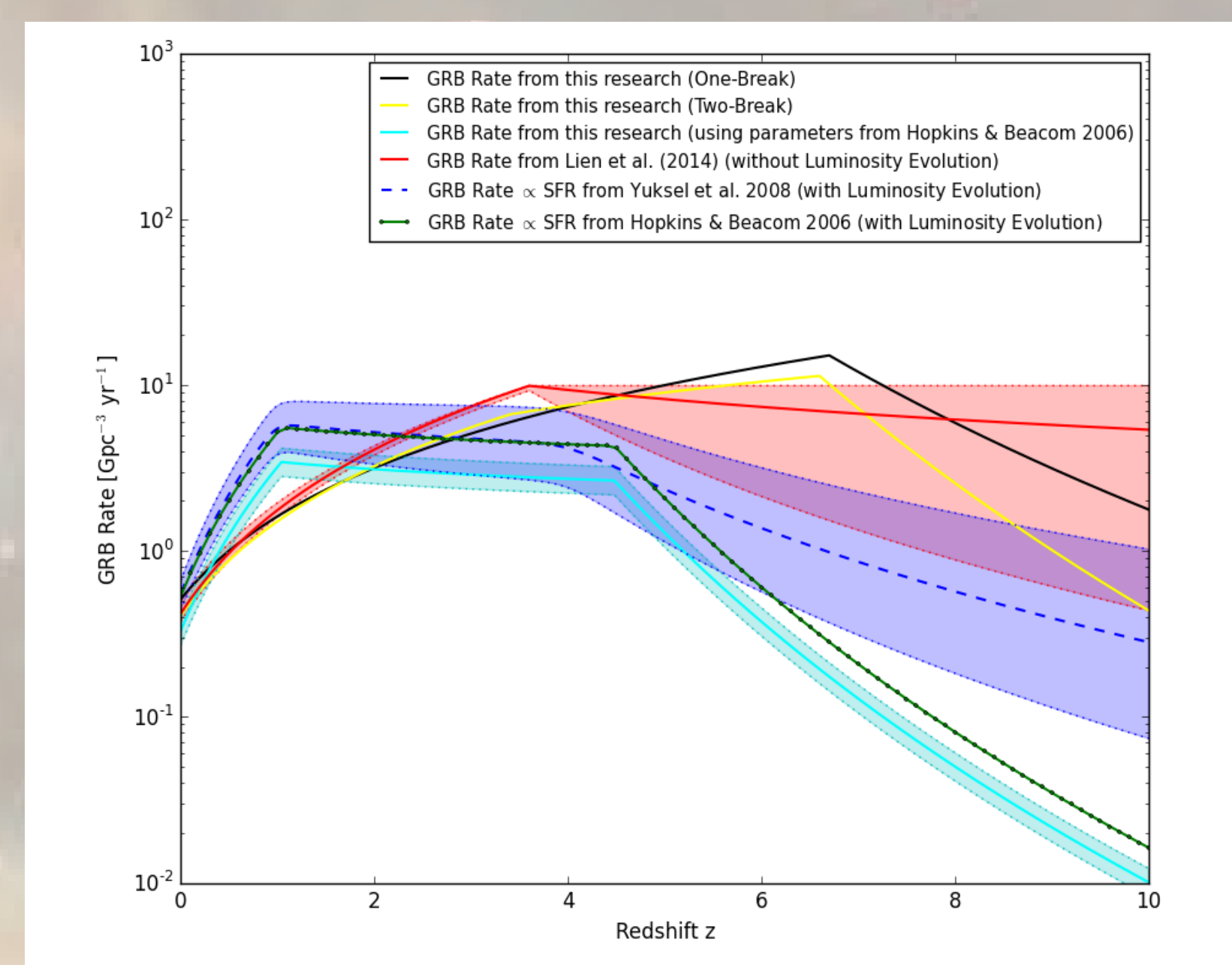


Figure 8: Comparison of the GRB Rate models